A superconductor made by a metal heterostucture at the atomic limit tuned at the 'shape resonance': MgB$_2$*

A Bianconi[1,3]**, D Di Castro**[1]**, S Agrestini**[1]**, G Campi**[1]**, N L Saini**[1]**,
A Saccone**[2]**, S De Negri**[2] **and M Giovannini**[2]

[1] Unità INFM and Dipartimento di Fisica, Università di Roma 'La Sapienza', P le Aldo Moro 2,
00185 Roma, Italy
[2] Dipartimento di Chimica e Chimica Industriale, Università di Genova, Via Dodecaneso 31,
16146 Genova, Italy

E-mail: antonio.bianconi@roma1.infn.it

Abstract
We have studied the variation of superconducting critical temperature T_c
as a function of charge density and lattice parameters in $Mg_{1-x}Al_xB_2$
superconducting samples. The AB_2 heterostucture of metallic boron layers
(intercalated by A = magnesium, aluminum layers, playing the role of spacers)
is made by direct chemical reaction. The spacing between boron layers and
their charge density are controlled by chemical substitution of Mg by Al atoms.
We show that high T_c superconductivity is realized by tuning the chemical
potential at a 'shape resonance' according with the patent for 'high-temperature
superconductors made by metal heterostructures at the atomic limit'. The
energy width of the superconducting shape resonance is found to be about
400 meV.

The material design of heterostructures is reaching the atomic limit for engineering the
electronic, transport [1] and optical [2] properties of materials. The electronic energy
levels, wavefunctions and band structure of new materials can now be designed by quantum
engineering. The basis of quantum engineering is the control of the quantum confinement of
the electron gas in mesoscopic units to obtain artificial discrete electronic states in potential
quantum wells (i.e., the classical quantum effects for a particle in a box). While most
of the interest has been focused on semiconductor heterostructures, now the interest is
shifting to metallic heterostructures in order to design and tailor in unprecedented ways the

---

* For further information: http://www.superstripes.com/
[3] Corresponding author.

superconducting properties [3]. The size of the mesoscopic units in these heterostructures is of the scale of the Fermi wavelength $\lambda_F = 2\pi/k_F$ (where k_F is the wavevector of electrons at the Fermi level). While in a typical semiconductor heterostructure, as gallium arsenide at room temperature, the Fermi wavelength λ_F is of the order of ~ 25 nm, in a metallic heterostructure λ_F reaches the atomic limit in the range ~ 0.3–1.5 nm. The atomic monolayers provide the thinnest possible metallic slabs (also called quantum wells) where the electronic charge is delocalized over an effective thickness L^* of the order of the Fermi wavelength [4]. A superconducting heterostructure [5] is made by a superlattice of quantum wells of a first material B intercalated between a second material, A, that provides a periodic potential barrier for the electrons in the first material. The units BA are repeated a large number of times to form a superlattice ... BABABA ... with period λ_p. A superlattice of atomic monolayers can be realized by planes (with a bcc or hcp, or fcc, or honeycomb crystallographic lattice) of atoms B alternated with other planes (with a different bcc or hcp, or fcc, or honeycomb crystallographic lattice) of atoms A rotated with respect to each other to get lattice matching [6]. Stable pseudomorphic lattices of A or B materials appear in the heterostructures that are not stable in the separated homogenous materials. The internal stress due to lattice mismatch between the A and B intercalated layers induces a local micro-strain on each layer. The anharmonicity of lattice dynamics and multi-phonon interaction in the metallic layers are controlled by the micro-strain.

The growth of artificial metallic quantum superlattices at the atomic limit has been delayed by the technical problems for epitaxial growth of thin homogenous films with sharp interfaces at the atomic limit. In fact, the metallic thin films, grown by standard evaporation methods, get *disordered* on an atomic scale or *granular* on a mesoscopic scale and electrons get *localized* at low temperature.

Atomically perfect superlattices can be grown by direct chemical synthesis of elemental atoms A and B in optimized thermodynamic conditions. The superlattices of quantum wells at the atomic limit shown in figure 1 have been known since 1935 as the AlB$_2$ crystallographic structure [7–10]. Let us consider the case of A = aluminum or magnesium and B = boron;
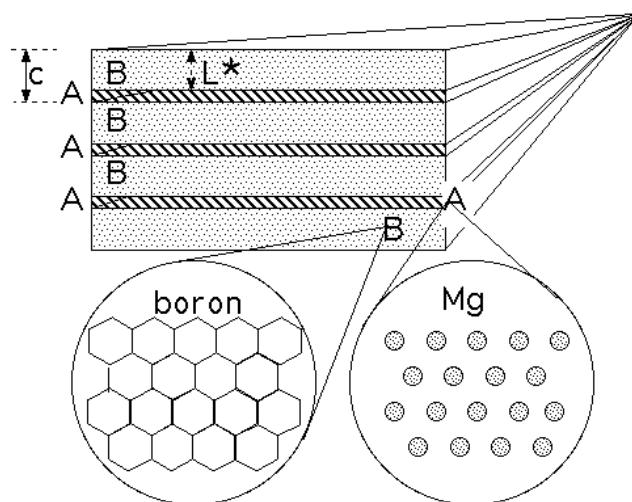

Figure 1. Pictorial view of the superlattice of metallic boron monolayers (B) made of graphite-like honeycomb lattice separated by hexagonal Mg layers (A) forming a superlattice ABAB in the *c*-axis.

these two elements do not mix in the solid phase and the radius of B is much smaller than the radius of A = Mg (Be or Al). However at high temperature (T = 1223 K) Mg atomic gas diffuses inside the boron crystals and a superlattice of pseudomorphic honeycomb graphite-like boron monolayers with intercalated hexagonal, Mg (Al, or Be), monolayers is formed.

The use of this type of metallic superlattice as superconductors at high temperature to overcome the technical limitation of cuprate perovskites and standard superconducting Nb alloys has been described in a patent [11] that discloses how the superconducting temperature can be amplified by a large factor. The amplification is achieved in a superlattice of quantum metallic wells by tuning the chemical potential (the Fermi energy E_F) at a 'shape resonance' occurring near the quantum critical point (QCP) [12–22] at energy E_c for a 2D–3D transition near the threshold (bottom or top) of the 2D subbands of the superlattice. The superconducting critical temperature (T_{cn}) is amplified by an amplification factor f of the order of 100–1000 from the low temperature range to the high temperature range by tuning the Fermi energy over an energy range $|E_c - E_F| < \Delta_0$, with $\Delta_0 > t_z$, where t_z is the small electron hopping energy between the boron layers.

It was known that in the AlB$_2$-type diborides the electronic structure of the boron superlattice is formed by two dimensional (2D) boron $\sigma(2p_{x,y})$ subbands that coexist with other 3D π (2p$_z$) bands crossing the Fermi level [23]. Near the top of the 2D boron $\sigma(2p_{x,y})$ subband, as shown in figure 2, the characteristic QCP of the superlattice occurs at the energy E_c at the Γ point where a transition to the 3D regime occurs for $E > E_c$ up to the top of the subband at A point. The electrons in the B $\sigma(2p_{x,y})$ subband have cylindrical Fermi surface in the energy range $E_F < E_c$ where hopping between the metallic units in the transversal direction is not allowed and a closed 3D Fermi surface in the energy range at $E_c < E_F < E_c + 4t_z$ (see figure 3) where hopping between the metallic layers is allowed, giving a small dispersion perpendicular to the metallic layers with bandwidth $4t_z$.
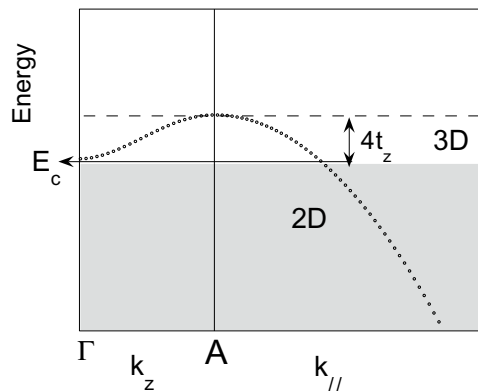

Figure 2. The superconducting nth shape resonance occurs near the quantum critical point at energy E_c at the top of a single particular hole-like subband of the electronic structure of a superlattice of quantum wells where the partial electronic structure of this subband shows a dimensional transition from 2D at $E < E_c$ to 3D in the range $E_c < E < E_0$.

According to [11] the high T_c superconductors can be made by diborides if the chemical potential is tuned for T_c amplification in the energy range $|E_c - E_F| < \Delta_0$. The 'shape resonance' can be obtained by tuning the energy level E_F (via changes of the charge density) and/or tuning the energy position of E_c (via changes of the lattice parameters of the superlattice). The difficulty in reaching the resonance point is due to the fact that the resonance is very narrow. Therefore both the lattice parameters and the charge density of metallic monolayers have to
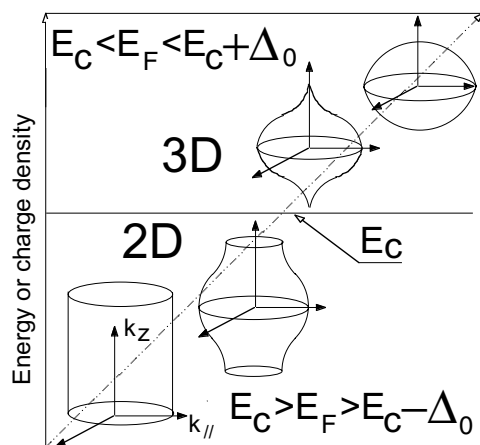
Figure 3. Pictorial view of the transition in a particular subband of a superlattice of quantum wells, from a 2D-like Fermi surface below E_c to a 3D-like Fermi surface above E_c. The shape resonance for the superconducting gap occurs in a energy range Δ_0 around E_c.

be controlled in a very fine scale ($\Delta_0 \ll E_F$ in good metals) for a fine tuning of the energy difference $\Delta = E_F - E_c$.

In most of the diborides the Fermi level is out of resonance $|E_F - E_c| > \Delta_0$ but in MgB_2 the Fermi level is close to E_c [23], therefore T_c is amplified according to the claims in [11]. MgB_2 was used as a component for chemical reactions but never tested for superconducting properties before January 2001, when it was shown to be a high T_c superconductor [24–26] with promising applications for energy transport and in electronics according to [11]. T_c reaches 40 K with an amplification of a factor $f \sim 100$ in MgB_2 in comparison with other diborides where $T_c < 0.4$ K. The shape resonance occurs for critical values of the lattice parameters (a and c that control the position of E_c) and of the charge density (that controls E_F) [27].

Here we report an investigation of the high T_c superconducting phase in MgB_2 by changing both the charge density and the superlattice structural parameters. In order to tune the chemical potential E_F around the quantum critical point at E_c in the energy range $|E_F - E_c| < 400$ meV we have used the chemical substitution of Mg by Al atoms in the $Mg_{1-x}Al_xB_2$ samples [28]. We show that high T_c superconductivity is realized at a 'shape resonance' by tuning the chemical potential within an energy range $\Delta_0 = 400$ meV from the QCP.

The powder $Mg_{1-x}Al_xB_2$ samples have been synthesized by direct reaction of the elements. The starting materials were elemental magnesium and aluminum (rod, 99.9 mass% nominal purity) and boron (99.5% pure <60 mesh powder). The elements in a stoichiometric ratio were enclosed in tantalum crucibles sealed by arc welding under argon atmosphere. The Ta crucibles were then sealed in heavy iron cylinder and heated for one hour at 800 °C and two hours at 950 °C in a furnace. The samples were characterized by x-ray diffraction and the lattice parameters were determined by standard least-squares refinement of the diffraction data recorded using the Cu Kα emission at room temperature. The Al doping in $Mg_{1-x}Al_xB_2$ samples controls (1) the spacing between the metallic boron layers (measured by the c-axis), (2) the in plane B–B distance (measured by the a-axis) and (3) the charge density that increases by x electrons per unit cell. The variations of the ratios $a(x)/a_0$ and $c(x)/c_0$ where c_0 and a_0 are the crystallographic axes in the undoped MgB_2 compound as a function of aluminum content x are plotted in figure 4. By increasing Al content x we observe a contraction of the spacing between the boron monolayers shown in figure 1 given by the variation of the c-axis. Figure 4 shows

that the variation of the a-axis with aluminum doping is much smaller than that of the c-axis as observed by the pressure effect [29]. The contraction of the a-axis measures the reduction of the micro-strain of the B–B distance with Al substitution [27]. The expected variations of the lattice parameters for a solid solution of AlB$_2$ and MgB$_2$ are indicated by the dashed lines. We observe a variation of the slope of both lattice parameters at aluminum content $x = 0.3$.
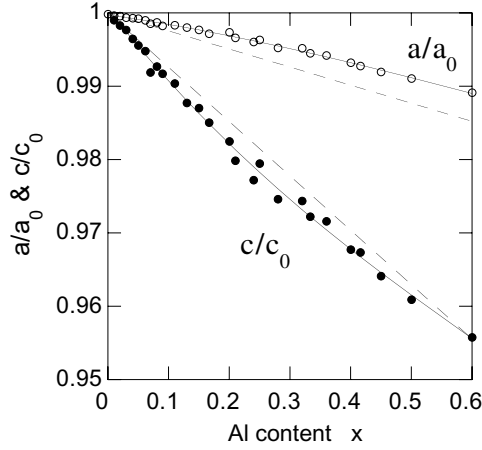

Figure 4. The variation of the ratios of a and c axes: $a(x)/a_0$ and $c(x)/c_0$ as a function of Al doping x (where a_0 and c_0 are the lattice parameters of the MgB$_2$ compound) in Mg$_{1-x}$Al$_x$B$_2$ samples.

The superconducting properties of Mg$_{1-x}$Al$_x$B$_2$ superconductors have been investigated by the temperature dependence of the complex conductivity using the single-coil inductance method [30]. This method is based on the influence of the sample on the radio frequency complex impedance of an LC circuit. Temperature-dependent measurements of the complex impedance, with and without the sample, allow extraction of the complex conductivity of the sample. The real part of the complex conductivity is related to the dissipative conductivity, while the imaginary part is a measure of the London penetration depth. Therefore, the temperature dependence of the imaginary part contains information about the superfluid density and dissipation effects in the vortex dynamics.

The sample was located in the vicinity of the coil. A sketch of the experimental circuit geometry is shown as an inset of figure 5, that shows the ratio of the square of resonant frequencies $f_0(T)^2/f(T)^2$ where $f_0(T)$, and $f(T)$, are the LC resonance frequency measured without and with the sample, respectively. Below the superconducting transition, the inductance L of the circuit decreases because of the screening sheet currents, and, hence, the resonant frequency $f(T)$ shows a sharp increase. Therefore at the transition temperature T_c a sharp drop of the ratio $f_0(T)^2/f(T)^2$ is observed, that is a good probe of the superconducting transition. The derivative of $f_0(T)^2/f(T)^2$ is shown in the upper panel of figure 5 and the derivative maximum has been used to define T_c. The results show that we have succeeded in changing by aluminum doping two key parameters that control the critical temperature: (1) the charge density, that has been increased up to 0.5 electrons/cell, raising the chemical potential $E_F(x)$; (2) the lattice parameters c and a that control the energy shift of $E_c(x)$ in the electronic structure of the superlattice of boron monolayers,

According with band structure calculations for Mg$_{1-x}$Al$_x$B$_2$ at $x = 0$ in the pure system the Fermi level E_F is in the 2D regime at 395 meV below the QCP of the σ 2p$_{x,y}$ band at E_c. The 3D regime occurs over an energy range $4t_z = 368$ meV above E_c. The decrease of the
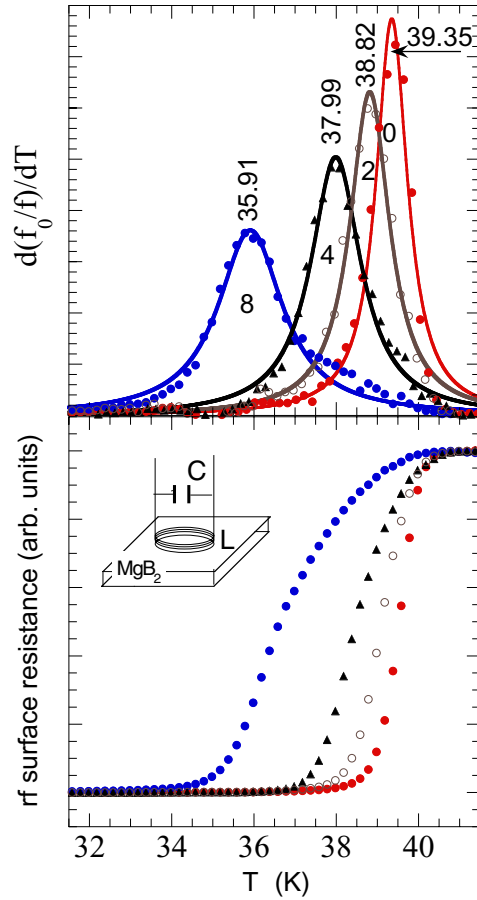
Figure 5. Lower panel, the radio frequency surface resistance probed by the ratio $f_0(T)^2/f(T)^2$ of the probing LC circuit of $Mg_{1-x}Al_xB_2$ samples. The inset shows a schematic diagram of the experimental system. Upper panel, the peak of the derivative of the ratio $f_0(T)^2/f(T)^2$ at T_c.

a-axis, $a(x)$, shown in figure 4 pushes to higher energy the position of the critical point $E_c(x)$ at Γ. The decrease of the c-axis with Al doping shown in figure 4 increases the dispersion perpendicular to the metallic boron monolayers t_z and decreases the position of $E_c(x)$. The position of the Fermi level $E_F(x)$ changes with x due to changes both of the electron counts and of the density of states. At aluminum doing $x = 0.5$ the σ $2p_{x,y}$ is nearly filled and the Fermi level is in the 3D regime above the QCP at $\Delta(0.5) = E_c(0.5) - E_F(0.5) = -320$ meV [23]. Therefore by aluminum doping in the range $0 < x < 0.5$ it is possible to test the variation of the critical temperature at the shape resonance by changing the chemical potential in the range $320 < \Delta(x) < 395$ meV.

In figure 6 we report the variation of the critical temperature as a function of the energy shift of the chemical potential with Al doping x. The energy shift of the chemical potential $\Delta(x)$ as a function of the aluminum doping x has been obtained by Massidda *et al* from their band structure calculations [23].

The critical temperature follows qualitatively the density of states as expected for a shape resonance [18, 19]. The high T_c occurs by tuning the Fermi level over a range $\Delta_0 = 400$ meV above and below the QCP at E_c. High critical temperature 23 K $< T_c < 40$ K occurs for
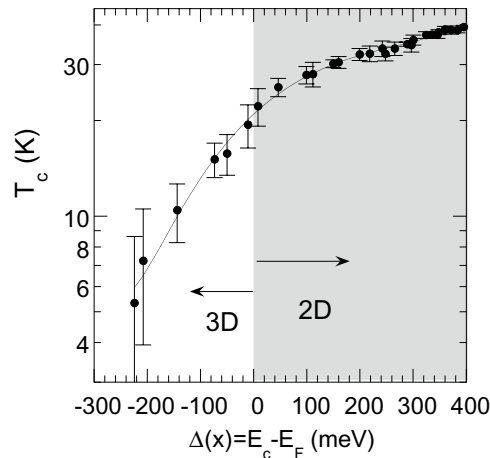
Figure 6. The critical temperature T_c as a function of the shift of the chemical potential $\Delta(x) = E_c(x) - E_F(x)$, where E_F is the Fermi level and E_c the QCP of the boron σ $2p_{x,y}$ band, where a 2D to 3D transition occurs, as a function of Al doping x.

$E_F < E_c$ in the 2D regime and the low critical temperature 5 K $< T_c <$ 13 K occurs in the 3D range for $E_c < E_F$.

In conclusion we have shown that the MgB$_2$ superconductor with high critical temperature, in accordance with [11], is characterized by being formed by a plurality of first portions formed of first layers (of graphite-like structure) made by a first superconducting material (boron), alternated with second portions formed by second layers (of hexagonal structure) made of a second material (magnesium) with different electronic structure; the said first portions being formed of first layers having a thickness L, and the said second portions being formed by second layers having a thickness W, with a period $L + W = c$ such as to tune the Fermi level to a 'shape resonance' of the superlattice. The high critical temperature is achieved by tuning the chemical potential relative to the QCP at E_c for a 2D to 3D transition in the σ $2p_{x,y}$ by changing both the lattice parameters and the charge density in Mg$_{1-x}$Al$_x$B$_2$.

The width of the shape resonance has been found to be of the order of 400 meV larger than the transverse band dispersion $4t_z$ and several times the energy of the E$_{2g}$ phonon in the range of 600–800 cm^{-1}. This can be associated with strong anharmonic effects due to the large micro-strain of the B–B distance in the metallic boron layers [27] as in cuprates [31]. These results imply a pairing mechanism mediated by many phonons and coupled with electronic excitations where the chemical potential is tuned at a shape resonance [11]. The high T_c in MgB$_2$ shows up in a narrow regime near critical values of the lattice parameters of the superlattice at the atomic limit and at a critical density according to [11], therefore other new heterostructures at the atomic limit of similar type could be synthesized by chemical reactions to get higher T_c via the shape resonance effect with the possibility of reaching room temperature superconductors.

Acknowledgments

delle Ricerche (CNR); (ii) Istituto Nazionale di Fisica della Materia (INFM) and (iii) the Ministero dell'Università e della Ricerca Scientifica (MURST).

References

[1] Datta S 1996 *Electronic Transport in Mesoscopic Systems* (Cambridge: Cambridge University Press)
[2] Capasso F, Faist J and Sirtori C 1996 *J. Math. Phys.* **37** 4775
[3] Brooks M 1999 *New Sci.* **2192** 38
    Bianconi A 1998 *Phys. World* **11** 20
[4] Batra I P, Ciraci S, Scrivastava G P, Nelson J S and Fong C Y 1986 *Phys. Rev.* B **34** 8246
    Ciraci S and Batra I P 1986 *Phys. Rev.* B **33** 4294
[5] Ruggiero S T and Beasley M P 1985 *Synthetic Modulated Structures* ed L L Chang and B C Giessen (New York: Academic) p 365
[6] Himpsel F J 1991 *Phys. Rev.* B **44** 5966
    Ortega J E, Himpsel F J, Mankey G L and Willis R F 1993 *Phys. Rev.* B **47** 1540
    Mankey G L, Willis R F and Himpsel F J 1993 *Phys. Rev.* B **47** 190
    Segovia P, Michel E G and Ortega J E 1996 *Phys. Rev. Lett.* **77** 3455
[7] Hoffmann W and Jänicke W 1935 *Naturwiss.* **23** 851
    Hoffmann W and Jänicke W 1936 *Z. Physik. Chem.* B **31** 214
[8] Russel V, Hirst R, Kanda F and King A 1953 *Acta Crystallogr.* **6** 870
[9] Jones E and Marsh B 1954 *J. Am. Chem. Soc.* **76** 1434
[10] Duhart P 1962 *Ann. Chim.* **7** 339
[11] High T_c superconductors made by metal heterostructures at the atomic limit 1995 *International Patent* PCT WO 95/16281
    1998 *European Patent* 0733271
    Japanese Patent JP 286 8621
    web site http://www.superstripes.com/
[12] Bianconi A 1994 *Solid State Commun.* **89** 933
[13] Bianconi A, Missori M, Saini N L, Oyanagi H, Yamaguchi H, Ha D H and Nishiara Y 1995 *J. Supercond.* **8** 545
[14] Perali A, Bianconi A, Lanzara A and Saini N L 1996 *Solid State Commun.* **100** 181
[15] Perali A, Valletta A, Bardelloni G, Bianconi A, Lanzara A and Saini N L 1997 *Proc. 1st Int. Conf. on Stripes, Lattice Instabilities and High T_c Superconductivity (Rome, 1996) J. Supercond.* **10** 355–9
[16] Valletta A, Bardelloni G, Brunelli M, Lanzara A, Bianconi A and Saini N L 1996 *Proc. 1st Int. Conf. on Stripes and High T_c Superconductivity (Rome, 1996) J. Supercond.* **10** 383–7
[17] Bianconi A, Valletta A, Perali A and Saini N L 1997 *Solid State Commun.* **102** 369
[18] Valletta A, Bianconi A, Perali A and Saini N L 1997 *Z. Phys.* B **104** 707
[19] Bianconi A, Valletta A, Perali A and Saini N L 1998 *Physica* C **296** 269
[20] Bianconi A, Agrestini S, Bianconi G, Di Castro D and Saini N L 1998 *Stripes and Related Phenomena (Proc. 2nd Int. Conf. on Stripes and High T_c Superconductivity (Rome, 1998))* ed A Bianconi and N L Saini (New York: Kluwer–Plenum) pp 9–25
[21] Bianconi A 2000 *Proc. 3rd Int. Conf. Stripes and High T_c Superconductivity (Rome, 2000) Int. J. Mod. Phys.* B **14** 3289
[22] Saini N L and Bianconi A 2000 *Proc. 3rd Int. Conf. on Stripes and High T_c Superconductivity (Rome, 2000) Int. J. Mod. Phys.* B **14** 3649
[23] Satta G, Profeta G, Bernardini F, Continenza A and Massidda S 2001 *Preprint* cond-mat/0102358, references therein and private communication
[24] Nagamatsu J, Nakagawa N, Muranaka T, Zenitani Y and Akimitsu J 2001 *Nature* **410** 63
[25] Bud'ko S L, Lapertot S L, Petrovic C, Cunninghamy C E, Anderson N and Canfield P C 2001 *Phys. Rev. Lett.* **86** 1877
[26] Finnemore D E, Ostenson J E, Bud'ko S L, Lapertot G and Canfield P C 2001 *Phys. Rev. Lett.* **86** 2420
[27] Bianconi A, Saini N L, Di Castro D, Agrestini S, Campi G, Saccone A, De Negri S, Giovannini M and Colapietro M 2001 *Preprint* cond-mat/0102410
[28] Slusky J S *et al* 2001 *Nature* **410** 343
[29] Jorgensen J D, Hinks D G and Shortl S 2001 *Preprint* cond-mat/0103069
[30] Di Castro D, Saini N L, Bianconi A and Lanzara A 2000 *Physica* C **332** 405
[31] Bianconi A, Bianconi G, Caprara S, Di Castro D, Oyanagi H and Saini N L 2000 *J. Phys.: Condens. Matter* **12** 10 655